Bioorganic & Medicinal Chemistry 19 (2011) 7416–7424

Contents lists available at SciVerse ScienceDirect

Bioorganic & Medicinal Chemistry

journal homepage: www.elsevier.com/locate/bmc

Molecular insights into human monoamine oxidase (MAO) inhibition by 1,4-naphthoquinone: Evidences for menadione (vitamin K3) acting as a competitive and reversible inhibitor of MAO

Eduardo Coelho Cerqueira [a], Paulo Augusto Netz [b], Cristiane Diniz [a], Vanessa Petry do Canto [b], Cristian Follmer [a,*]

[a] Department of Physical Chemistry, Institute of Chemistry, Federal University of Rio de Janeiro, Rio de Janeiro 21941-909, Brazil
[b] Institute of Chemistry, Federal University of Rio Grande do Sul, Porto Alegre 91501-970, Brazil

ARTICLE INFO

Article history:
Received 12 August 2011
Revised 9 October 2011
Accepted 16 October 2011
Available online 20 October 2011

Keywords:
Monoamine oxidase
1,4-Naphthoquinone
Menadione
Docking
Flavin

ABSTRACT

Monoamine oxidase (MAO) catalyzes the oxidative deamination of biogenic and exogenous amines and its inhibitors have therapeutic value for several conditions including affective disorders, stroke, neurodegenerative diseases and aging. The discovery of 2,3,6-trimethyl-1,4-naphthoquinone (TMN) as a nonselective and reversible inhibitor of MAO, has suggested 1,4-naphthoquinone (1,4-NQ) as a potential scaffold for designing new MAO inhibitors. Combining molecular modeling tools and biochemical assays we evaluate the kinetic and molecular details of the inhibition of human MAO by 1,4-NQ, comparing it with TMN and menadione. Menadione (2-methyl-1,4-naphthoquinone) is a multitarget drug that acts as a precursor of vitamin K and an inducer of mitochondrial permeability transition. Herein we show that MAO-B was inhibited competitively by 1,4-NQ (K_i = 1.4 μM) whereas MAO-A was inhibited by non-competitive mechanism (K_i = 7.7 μM). Contrasting with TMN and 1,4-NQ, menadione exhibited a 60-fold selectivity for MAO-B (K_i = 0.4 μM) in comparison with MAO-A (K_i = 26 μM), which makes it as selective as rasagiline. Fluorescence and molecular modeling data indicated that these inhibitors interact with the flavin moiety at the active site of the enzyme. Additionally, docking studies suggest the phenyl side groups of Tyr407 and Tyr444 (for MAO-A) or Tyr398 and Tyr435 (for MAO-B) play an important role in the interaction of the enzyme with 1,4-NQ scaffold through forces of dispersion as verified for menadione, TMN and 1,4-NQ. Taken together, our findings reveal the molecular details of MAO inhibition by 1,4-NQ scaffold and show for the first time that menadione acts as a competitive and reversible inhibitor of human MAO.

© 2011 Elsevier Ltd. All rights reserved.

1. Introduction

Monoamine oxidases [amine: oxygen oxidoreductase (deamination) (flavin containing) EC 1.4.3.4.] catalyze the oxidative deamination of biogenic amines, including neurotransmitters and exogenous amines such as the neurotoxin 1-methyl-4-phenyl-1,2,3,6-tetrahydropyridine (MPTP).[1–3] Two isoforms of MAO have been identified: MAO-A and MAO-B.[4] Abnormal activity of the MAO-B isoform has been linked to neurological disorders including Parkinson's disease (PD) and Alzheimer's disease (AD),[5,6] whereas the MAO-A isoform appears to be associated with psychiatric conditions including depression and cardiac cellular degeneration.[7–9] Additionally, previous studies have reported that the level of MAO-B in humans increases four- to five-fold during aging and leads to an increase in catalytic reaction products such as hydrogen peroxide and a reduction in certain neurotransmitter levels.[10] The MAO-A level was significantly higher in the hearts of aged rats and has been identified as being involved in cardiac cellular degeneration. These observations make MAO-A an important target in the development of cardioprotective agents.[9] Unfortunately, the utilization of MAO inhibitors might be limited, in some cases, by side effects such as those associated with the co-administration of certain foods or drugs, which can result in dangerous hypertensive and hyperpyretic crises.[11] In light of these findings, enormous efforts have been undertaken to identify new pharmacophores that are associated with MAO inhibition.

It was reported that 2,3,6-trimethyl-1,4-naphthoquinone (TMN), a component of flue-cured tobacco leaves and smoke, is a competitive inhibitor of MAO-A and MAO-B that exhibits protective properties against MPTP toxicity in mice.[12,13] MAO-B converts MPTP to MPP+, which causes parkinsonism in various animal models, including human and non-human primates.[3,14] This finding suggests that naphthoquinones may be important pharmacophores for acting on

* Corresponding author. Tel.: +55 21 2562 7752; fax: +55 21 2562 7265.
E-mail address: follmer@iq.ufrj.br (C. Follmer).

0968-0896/$ - see front matter © 2011 Elsevier Ltd. All rights reserved.
doi:10.1016/j.bmc.2011.10.049

monoamine oxidase inhibition. Naphthoquinones are widespread in nature and have been found in higher plants, fungi and actinomycetes.[15] The 1,4-naphthoquinone (1,4-NQ) scaffold is often found in bioactive molecules, such as vitamin K. By using biochemical and computational approaches we investigate the molecular details of the inhibition of MAO by 1,4-NQ comparing it with the bioactive 1,4-NQ derivatives: menadione and TMN.

2. Experimental

2.1. MAO assay

Microsomes from baculovirus-infected insect cells that express recombinant human MAO-A and MAO-B were purchased from Sigma-Aldrich. The activity of MAO-A and MAO-B were evaluated by a fluorometric assay that measures the amount of resorufin produced from Amplex Red® (AR) (Invitrogen) in the presence of hydrogen peroxide (generated by MAO action) and horseradish peroxidase (HRP).[16] These assays were carried out in a 96-well microplate. The fluorescence intensity was measured by a fluorescence microplate reader in a Cary Eclipse Fluorimeter (Varian Inc) with excitation at 571 nm and emission at 585 nm. The effect of the inhibitors on the fluorescence emission at 585 nm was previously evaluated, and a correction was performed when necessary. The reaction mixture (final volume of 200 μL) contained 5 μg/mL MAO-A or MAO-B in a 50 mM sodium phosphate buffer of pH 7.4, 1 mM p-tyramine (MAO-A and MAO-B substrate) or 1 mM benzylamine (MAO-B substrate), 1 U/mL HRP and 200 μM AR. This mixture were incubated at 37 °C for 45 min in the presence or absence of the inhibitors. The enzyme plus the inhibitor were incubated at 37 °C for 20 min prior to the addition of the substrate, HRP and AR. The inhibitors were dissolved in 100% DMSO, and equivalent concentrations of DMSO alone (1–2%) were used as controls. Clorgyline (MAO-A inhibitor) or pargyline (MAO-B inhibitor) were used at a concentration of 5 μM and served as a positive control for inhibition. To verify whether the inhibitors affect the enzymatic assay by inhibiting the AR oxidation by HRP or by scavenging the hydrogen peroxide that was generated, hydrogen peroxide was preincubated in the presence or absence of the inhibitors, and 1 U/mL HRP, 1 mM substrate and 200 μM AR were added to the reaction mixture. This mixture was incubated at 37 °C for 45 min, and the resorufin content was determined by fluorescence, as described above. The fluorescence intensity values were converted to amount of hydrogen peroxide formed by using a calibration curve. The enzymatic activity was expressed as nanomoles of hydrogen peroxide produced per milligram of enzyme each minute at pH 7.4 and 37 °C.

2.2. Kinetic parameters

To evaluate the mechanism of inhibition of MAO-A and MAO-B, the effect of the inhibitors (1,4-NQ and menadione) on the Michaelis-Menten constant (K_m) and maximum reaction rate (V_{max}) values was obtained by plotting the data according to the Lineweaver-Burk method. The K_i value for the inhibition of MAO by menadione or 1,4-NQ was determined from the double reciprocal plot: 1/rate of formation ($1/V$) versus 1/substrate concentration (50, 75, 100, 150 and 250 μM) in the presence of varying concentrations of menadione or 1,4-NQ (1, 2, 3, 5 and 8 μM). The K_i value was calculated from the interception of the curves obtained by plotting $1/V$ versus the inhibitor concentration for each substrate concentration.[17] Additionally, the K_i value was estimated by plotting the slope of each Lineweaver-Burk plot versus the inhibitor concentration.

2.3. Reversibility of the inhibition

To investigate the reversibility of the inhibition, MAO-A or MAO-B (50 μg/mL) was incubated with 100 μM of the inhibitor at 37 °C for 20 min and then dialyzed for 3 h at 4 °C against a 50 mM sodium phosphate buffer at pH 7.4 containing 25 mM sucrose, 0.1 mM EDTA and 5% glycerol. The maximum rate (V_{max}) and the K_m, before and after the dialysis, were obtained by plotting the data according to the Lineweaver-Burk method using a final concentration for the enzyme and the inhibitors of 5 μg/mL and 5 μM, respectively.

2.4. Spectroscopy

The interaction of the inhibitor with the flavin adenosine dinucleotide (FAD) cofactor of MAO-B was investigated by exploiting the fluorescence properties of the flavin group as previously described.[18] MAO-B (5 μg/mL) was incubated in the presence of 2–100 μM of the inhibitor or an equivalent amount of DMSO, and the fluorescence spectra was recorded in a Cary Eclipse Fluorimeter (Varian Inc) with excitation at either 412 nm (emission at 470–540 nm) or 450 nm (emission at 520–560 nm).

2.5. Molecular modeling: ligand and receptor building

The structure of menadione, 1,4-naphthoquinone and TMN were built with *GaussView*[19] and optimised with RHF/6-31G (d,p) using GAUSSIAN 98.[20] The final structures were converted to the *mol2* format. The corresponding Gasteiger-Marsili charges[21] were calculated using *Babel*. The structures and charges were used without further modification as the ligand input files for *AutoDockTools*.[22] The MAO-B receptor structure was built as a modification of the structure obtained from the Protein Data Bank (PDB: 2VRL).[23] This structure contains a dimeric form of the human monoamine oxidase B, with each chain interacting with FAD and toluene. For docking purposes, only the coordinates of chain A and FAD were considered as the receptor structure, without toluene or hydration by water. The MAO-A receptor structure was also built as a modification of the structure obtained from the Protein Data Bank (PDB: 2Z5Y).[24] This structure includes a monomeric form of MAO-A with FAD and harmine (HRM, 7-methoxy-1-methyl-9*H*-beta-carboline). For docking purposes, only the coordinates of the protein and FAD were used as the receptor structure.

2.6. Molecular modeling: grid and docking

The grid box was built with a resolution of 0.375 Å and $70 \times 60 \times 70$ points and constituted a large region surrounding the interaction site close to FAD, inside the enzymes. The docking was carried out by *AutoDock 4.0*[25,26] with a Lamarckian Algorithm (Genetic Algorithm combined with a local search). The following parameters were chosen: 100 GA runs, population size of 50, 50,000,000 evaluations, 27,000 number of generations, maximum number of top individuals of 1, gene mutation rate of 0.02 and a crossover rate of 0.8. The *AutoDock 4.0* default values were used for the remaining docking parameters, except for the step size parameters that were chosen to be 0.2 Å (translation) and 5.0 degrees (quaternion and torsion). The docked conformations were clustered according to their geometrical similarity (rms of 2.0 Å) and docked energy. The interactions between the ligand and protein residues were analyzed with *AutoDock Tools*.[22]

3. Results and Discussion

3.1. MAO is reversibly inhibited by 1,4-NQ and menadione

The chemical structures of 1,4-NQ, menadione and TMN are shown in Figure 1. The effect of 1,4-NQ or menadione on MAO activity was evaluated by an extremely sensitive method that monitors the amount of hydrogen peroxide that is generated as a result of MAO-catalyzed reactions. These compounds have been shown not to alter the enzymatic method by either quenching resorufin fluorescence or acting as scavengers of the hydrogen peroxide that was produced. Therefore, all compounds tested (up to a concentration of 100 μM) did not affect the formation of resorufin from AR in presence of hydrogen peroxide (data not shown). The inhibitory effect of 1,4-NQ and menadione on MAO was evaluated by the Lineweaver-Burk plot in the presence of varying concentrations of the inhibitor. Figure 2A and B show that MAO-B was strongly inhibited by 1,4-NQ (K_i = 1.5 μM) and menadione

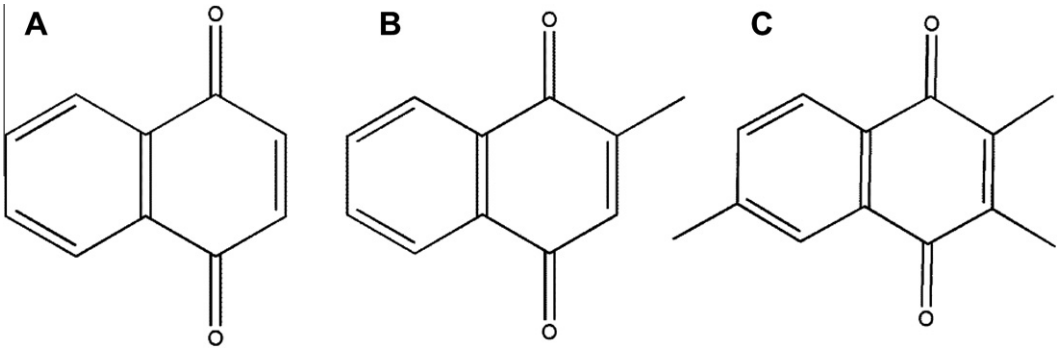

Figure 1. Chemical structures of 1,4-NQ (A), menadione (B) and TMN (C).

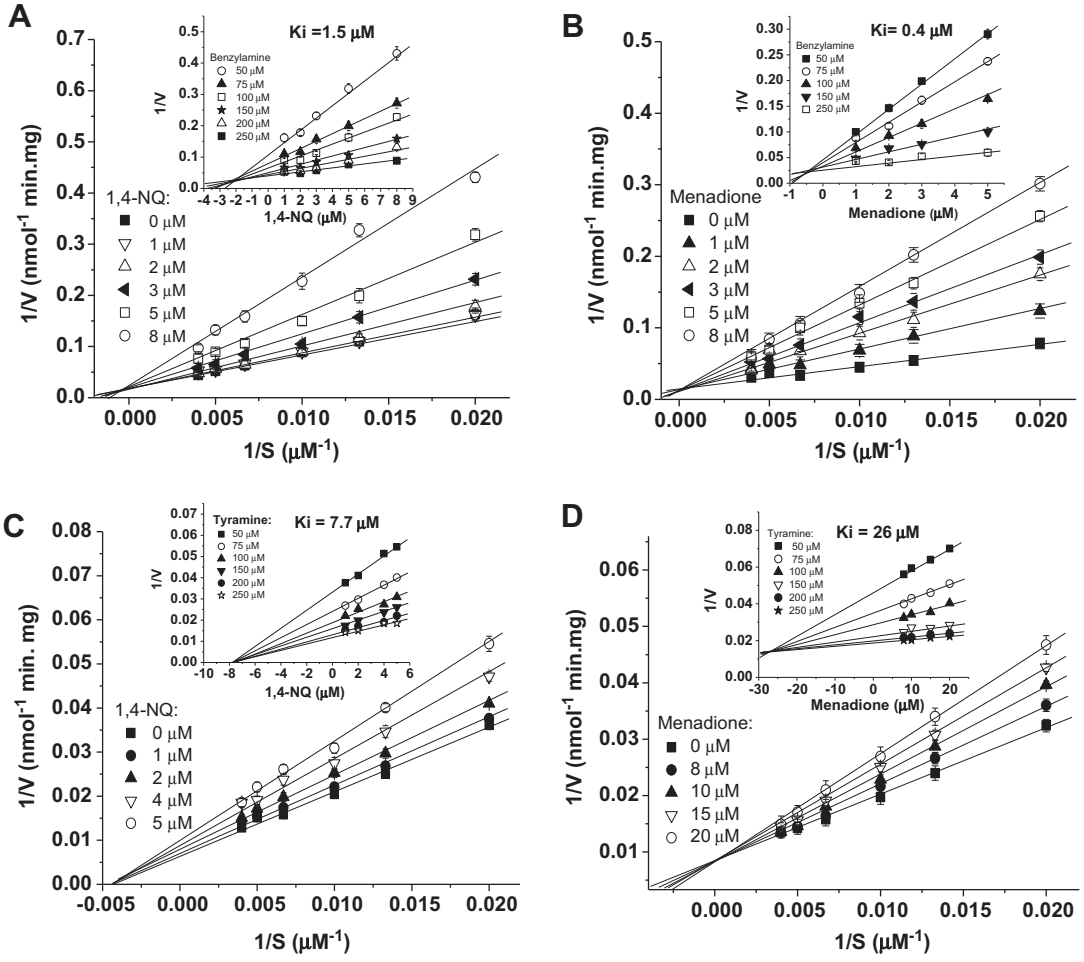

Figure 2. Kinetics of MAO inhibition by 1,4-NQ and menadione. The effect of the inhibitors on MAO was determined from the double reciprocal plot of 1/rate (1/*V*) versus 1/substrate concentration in presence of varying concentrations of 1,4-NQ or menadione on MAO-B (A and B, respectively) and on MAO-A (panels C and D, respectively). The K_i values were calculated by the intersection of the curves obtained by plotting 1/*V* versus the inhibitor concentration for each substrate concentration (insets). The data are presented as the mean of three experiments ± SD.

(K_i = 0.4 μM), respectively, in a concentration-dependent manner and this occurs by a competitive mechanism. Although MAO-A is inhibited by both 1,4-NQ and menadione, the K_i values of approximately 7.7 and 26 μM for 1,4-NQ and menadione, respectively, suggest that this isoform is less susceptible to inhibition than MAO-B (Fig. 2C and D). In addition, 1,4-NQ does not alter the K_m value of MAO-A, suggesting a noncompetitive mechanism for the inhibition.

Herein we demonstrate for the first time a link between menadione and MAO-B. The K_i value obtained for MAO-B and menadione is in the same range of that observed for others competitive inhibitors such as safinamide or coumarin analogs, with K_i values between 0.1 and 0.5 μM,[27] or norharman (beta-carboline), a reversible inhibitor of MAO-B found in tobacco (K_i of ~1.2 μM).[28] Menadione (vitamin K3) is a synthetic chemical compound that acts as a precursor of various forms of vitamin K. Additionally, menadione triggers oxidation of endogenous pyridine nucleotides and induces mitochondria permeability transition (MPT), this latter a result of the oxidative stress produced by the semiquinone radical formed by the interaction of menadione with the respiratory chain.[29] Since the oxidative catabolism of menadione is not catalyzed by MAO-B, it has been postulated that MAO-B activity is not involved in the MPT induced by menadione.[30] An important question that remains obscure is if and how the inhibitory activity of menadione on MAO-B might affect the MPT induced by menadione.

The determination of K_m and V_{max} values for MAO, in the presence or absence of the inhibitors, before and after dialysis, demonstrate the reversibility of the inhibition of MAO by 1,4-NQ or menadione (Table 1). In concordance with a competitive mechanism for the inhibition, both 1,4-NQ and menadione produced an increase in the K_m value from 0.15 mM to 0.75–0.85 mM for MAO-B, whereas the V_{max} remained unchanged (65–78 nmol min^{-1} m^{-1}). Menadione at a concentration of 5 μM produced a slight increase in the K_m for MAO-A with no alteration in V_{max} value, which is consistent with a competitive mechanism for the inhibition. In contrast, 1,4-NQ reduced the V_{max} for MAO-A, with no alteration in K_m, providing evidence for a noncompetitive inhibition. The enzyme incubated in the presence of the inhibitors and submitted to dialysis has its activity recovered, resulting in a decrease in K_m values for the competitive inhibitors and an increase in V_{max} for MAO-A and 1,4-NQ after the dialysis procedure. The slight reduction in V_{max} values for the enzymes after the dialysis procedure, in presence or absence of inhibitors, might be explained by the low stability of microsomes containing MAO during the dialysis procedure. For instance, MAO activity is completely abolished when the dialysis was done in absence of glycerol, sucrose or EDTA. Taken together, these findings indicate that the inhibition of MAO-A or MAO-B by 1,4-NQ and menadione is a reversible process.

Both menadione and 1,4-NQ are redox agents and this property could affect the results depending on the conditions of the enzymatic assay. However, we have compelling evidence that the inhibitory activity of these compounds is due to their ability to alter the enzymatic activity and not an artefact related to the enzymatic assay used in our experiment. Firstly, TMN is not a redox agent but is capable of inhibiting MAO at a concentration similar to that of 1,4-NQ and menadione (Table 2).[12] Secondly, the inhibition is reversed by either increasing the substrate concentration (e.g., tyramine or benzylamine do not interfere with the redox properties of 1,4-NQ or menadione) or dialysis. In addition, in presence of exogenous hydrogen peroxide, the conversion of AR to resorufin occurs in presence of up 100 μM of 1,4-NQ or menadione, indicating that there is no inhibition of HRP, scavenging of the hydrogen peroxide or any effect related to the oxidation of AR. Finally, if the inhibition observed was resulted of the redox properties of 1,4-NQ or menadione affecting the enzymatic conditions (FAD, oxygen, hydrogen peroxide), both MAO isoforms would be inhibited at the same range.

Table 1
Kinetic properties of MAO-A and MAO-B incubated with 5 μM menadione or 1,4-NQ before and after dialysis

	MAO-A		MAO-B	
	K_m (mM)	V_{max} (nmol min^{-1} mg^{-1})	K_m (mM)	V_{max} (nmol min^{-1} mg^{-1})
Before dialysis				
Control	0.24 ± 0.03	132 ± 11	0.15 ± 0.05	72 ± 4
Menadione (5 μM)	0.35 ± 0.02	130 ± 13	0.75 ± 0.07	73 ± 5
1,4-NQ (5 μM)	0.24 ± 0.03	101 ± 7	0.85 ± 0.05	71 ± 6
After dialysis				
Control	0.24 ± 0.03	128 ± 15	0.25 ± 0.05	64 ± 2
Menadione (5 μM)	0.23 ± 0.03	126 ± 8	0.30 ± 0.05	62 ± 4
1,4-NQ (5 μM)	0.25 ± 0.03	129 ± 7	0.40 ± 0.05	61 ± 6

Table 2
Kinetic data of the inhibition of MAO by 1,4-NQ, menadione and TMN

	Inhibitory constant K_i (μM)	
	MAO-A	MAO-B
1,4-NQ	7.7 ± 1.2 (noncompetitive)	1.5 ± 0.4 (competitive)
Menadione	26 ± 4 (competitive)	0.4 ± 0.15 (competitive)
TMN[12]	3 (competitive)	6 (competitive)

3.2. Both menadione and 1,4-NQ quench the fluorescence of the MAO-B flavin

The mechanism of inhibition for menadione or 1,4-NQ on MAO-B, proposed based on the kinetic assays, was investigated by fluorescence measurements of MAO-B in presence of the inhibitors. The catalytically active form of MAO-B exists as a homodimer with one covalently-bound FAD cofactor per monomer, which is responsible for the fluorescent properties of MAO-B. The presence of the FAD cofactor in MAO-B results in two distinctive chromophores in the resting state of the enzyme; one chromophore exists at 412 nm due to the presence of oxidized FAD and one at 450 nm related to the presence of a persistent flavin semiquinone.[18] Inhibitors that interact at the active site usually modify the fluorescence properties of the FAD, thereby providing information about the mechanism of inhibition. Since limited data has been published describing the fluorescence properties of the MAO-A isoform and this isoform has demonstrated low susceptibility to the inhibitors, we chose to focus our spectroscopic studies only on MAO-B isoform. Figure 3A and B show the fluorescence emission of MAO-B (excitation at either 412 or 450 nm) in the presence of varying concentrations of 1,4-NQ or menadione, respectively. We observe that both 1,4-NQ and menadione quench the flavin emission at 480 nm and at 530 nm. We also observed a nonlinear relationship between the fluorescence decay and the inhibitor concentration for both inhibitors (Fig. 3C). For 1,4-NQ, the fluorescence emissions at both 480 and 530 nm decay at a similar rate, whereas this effect is more pronounced at the 480 nm emission (excitation 412 nm) for menadione. These findings suggest that the oxidized FAD, rather the flavin semiquinone, is more prone to interact with menadione than 1,4-NQ. The inhibitor concentration that reduces the fluorescence signal at 450 nm to 50% of the control was 10–12 and 20–25 μM for menadione and 1,4-NQ,

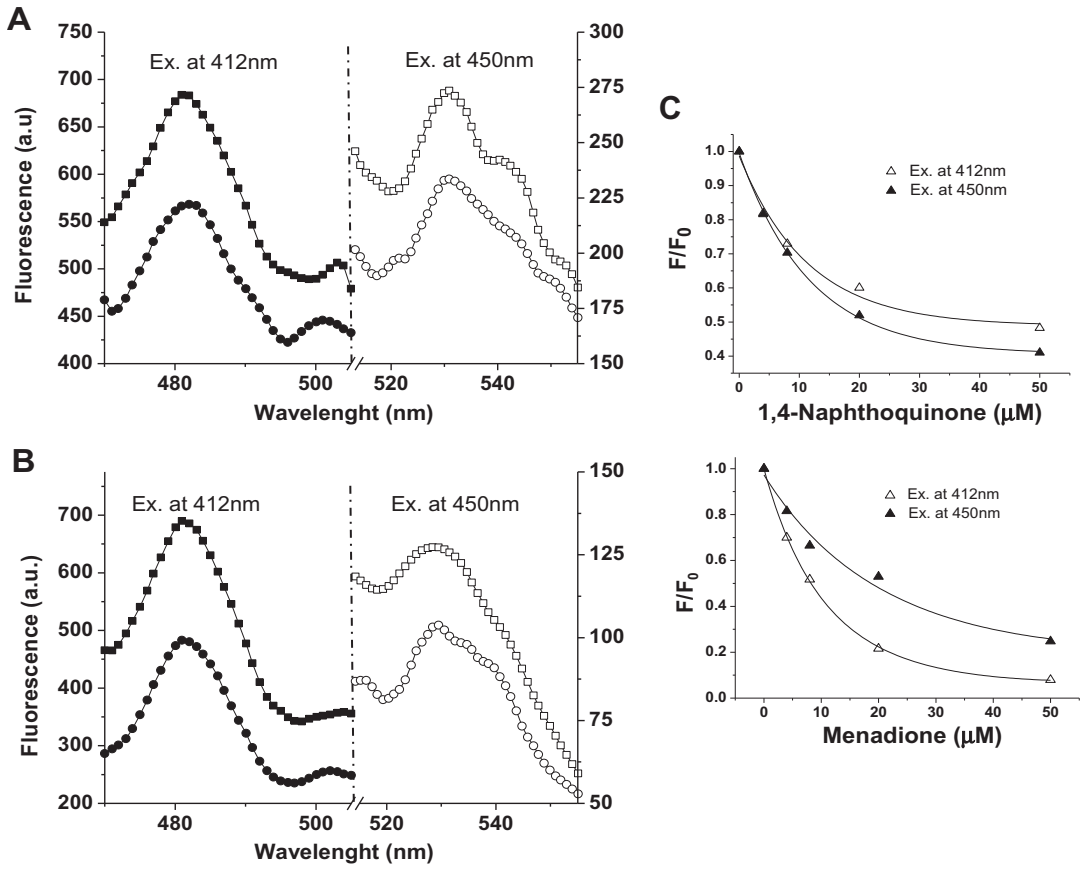

Figure 3. Evaluation of the fluorescence properties of MAO-B in the presence of menadione or 1,4-NQ. Panels A and B show the effect of 4 μM 1,4-NQ and menadione, respectively, on the fluorescence spectra of MAO-B (5 μg/mL) after excitation at 412 nm (filled symbols) or 450 nm (open symbols). The spectra were acquired at 25 °C in absence (■ and □) or presence (● and ○) of the inhibitors. Panel C shows the fluorescence signal normalised to the initial value (F/F_0) in varying concentrations of 1,4-NQ or menadione.

respectively, which is consistent with the inhibitory properties supported by the kinetic plots. The kinetic parameters of covalently bound MAO-B inhibitors, such as pargyline and selegiline, have been previously evaluated by the fluorescent properties of MAO-B without the need for a substrate.[18,31] Pargyline reduces the intensity at 530 nm, but the emission at 480 nm remains unchanged, suggesting that the oxidized flavin at the active site was modified by inhibitor binding.[18] Unfortunately, this procedure cannot be applied for reversible inhibitors. Taken together, these data suggest that both 1,4-NQ and menadione alter the properties of flavin fluorescence through an interaction with MAO-B residues in close proximity to the flavin moiety or through direct binding to flavin, which is consistent with the competitive mechanism observed in the kinetic studies.

3.3. Interaction of menadione or 1,4-NQ with MAO

Molecular docking studies were performed to evaluate the most probable conformations for the complex MAO-inhibitor. Unless specified, as in the case of hydrogen bond (HB), the interactions are classified as close contacts. Autodock uses an Amber-based force field to evaluate the free energy of binding, based on pairwise energetic terms and an estimate of the conformational entropy lost upon binding. The more negative is the binding free energy, the stronger is the interaction. The Table 3 shows the energy and the populations of the clusters generated in the docking. In menadione-MAO-B docking, the lowest energy conformation cluster represents 90% of all conformations obtained, and the lowest docking free energy was −5.50 kcal/mol. In this docked conformation, the menadione interacts with flavin moiety of the FAD site through a HB and displays close contacts with Gln206, Tyr326, Phe343, Tyr398 and Tyr435 (Fig. 4A). Similarities can be noted comparing our results with isatin (indol-2,3-dione), an endogenous MAO-inhibitor. For isatin, the indol ring is positioned between Tyr435 and Tyr398 residues in the hydrophobic cage with a perpendicular conformation to flavin ring of FAD cofactor,[32] similarly to observe for menadione and MAO-B. In the second lowest energy cluster (10% of the population), menadione interacts with residues on the enzyme surface and exhibits a lowest docking free energy of −2.93 kcal/mol.

In docking with MAO-A, menadione interacts with the residues in the active site in the lowest energy conformation cluster (61% of the conformers), exhibiting a lowest docking free energy of −5.40 kcal/mol. In this conformation, menadione binds to the flavin moiety through a HB and makes close contacts with Tyr69, Gln215, Leu337, Phe352, Tyr407 and Tyr444 (Fig. 4B). In the lowest energy conformation cluster, the energy of interaction of menadione with MAO-B was similar to that observed for menadione with MAO-A. However, this cluster represents 90% of the conformations generated for menadione and MAO-B, it is only 61% for menadione and MAO-A. This observation suggests competition with other sites for the interaction of menadione with MAO-A.

The energy of interaction between 1,4-NQ and MAO-A or MAO-B in the docked conformation of lowest energy was −4.90 kcal/mol and −5.15 kcal/mol, respectively. This docking occurred in the catalytic site of the enzymes. The interaction between MAO-B and

1,4-NQ is slightly different than the one observed between MAO-B and menadione; the interaction with Tyr326 is lost when menadione is replaced by 1,4-NQ, and a new interaction with Tyr60 takes place (Fig. 4C). Similarly to menadione, there is a remarkable preference for this cluster (95% of docked conformations) in MAO-B, which is not observed for MAO-A. For MAO-A, the kinetic data have demonstrated that 1,4-NQ inhibits the enzyme by a non-competitive mechanism, suggesting that other sites of interaction

Table 3
Docking of MAO-A or MAO-B with the inhibitors: 1,4-NQ, menadione and TMN

MAO-B inhibitor	Population, % total	Energy (kcal/mol)	Location
Menadione	90	−5.50	Active site: FAD (HB), Gln206, Tyr326, Phe343, Tyr398, Tyr435
	10	−2.93	Surface
1,4-NQ	95	−5.15	Active site: FAD (HB), Tyr60, Gln206, Phe343, Tyr398, Tyr435
	5	−2.73	Surface
TMN	88	−6.39	Active site: FAD (HB), Tyr60, Leu171, Tyr326, Phe343, Tyr398, Tyr435
	12	−3.31	Surface
MAO-A inhibitor			
Menadione	61	−5.40	Active site: FAD (HB), Tyr69, Gln215, Leu337, Phe352, Tyr407, Tyr444
	34	−5.14	Inner: Ile180, Asn181, Ile207, Phe208, Gln215, Ile335, Leu337, Met350, Phe352
	3	−5.06	Inner: Ile180, Phe208,Gln215, Ile335, Leu337, Met350, Phe352
	2	−4.19 to −3.13	Surface
1,4-NQ	60	−4.90	Active site: FAD (HB), Tyr69, Gln215, Phe352, Tyr407, Tyr444
	35	−4.63	Inner: Ile180, Phe208, Gln215, Ile335, Leu337, Phe352
	5	−3.90 to −3.50	Surface
TMN	65	−6.27	Active Site: FAD (HB), Tyr69, Gln215, Met350, Phe352, Tyr407,Tyr444
	35	−6.00	Inner: Ile180, Asn181, Phe208, Gln215, Cys323, Ile335, Leu337, Met350, Phe352

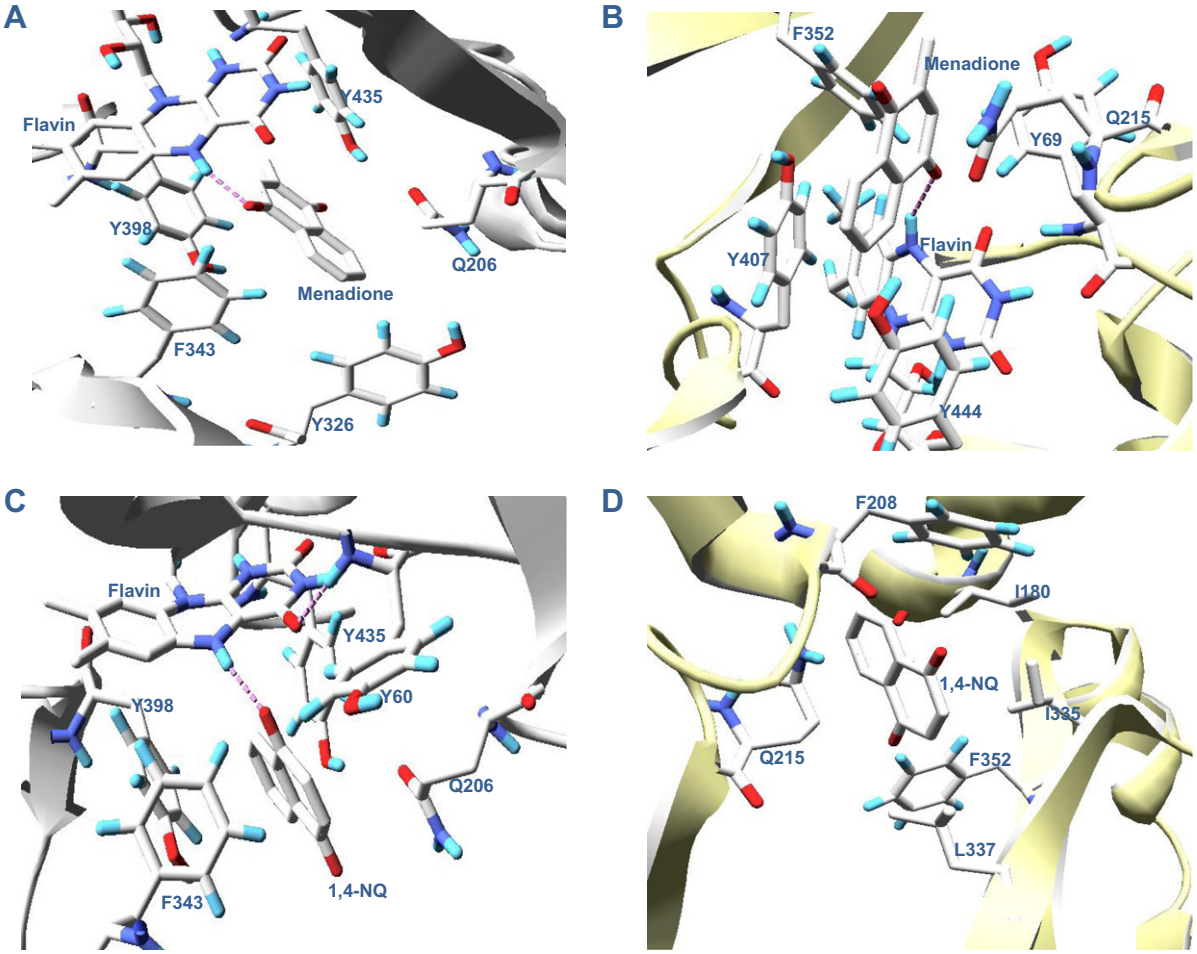

Figure 4. Probable interacting mode of menadione and 1,4-NQ with MAO. Panels A and B show the menadione interacting with particular residues at the active site of MAO-B and MAO-A, respectively, in the lowest energy docking conformation. In the interaction between MAO-B and 1,4-NQ, the inhibitor is docked similarly to menadione, with exception Tyr326, which is replaced by Tyr60 (C). In D, the second lowest energy docked conformation for 1,4-NQ and MAO-A is shown. In this conformation, the ligand interacts with interior residues of the enzyme instead of those in the catalytic site. This model is supported by kinetic data that indicate that 1,4-NQ inhibits the enzyme in a noncompetitive manner.

may be present. In the second lowest energy docked conformation for 1,4-NQ and MAO-A (4.63 kcal/mol) the ligand interacts with residues located in the inner portion of the enzyme (Ile180, Phe208, Gln215, Ile335, Leu337 and Phe352) instead of those in the catalytic site, which may explain the noncompetitive mechanism observed (Fig. 4D). For MAO-B and 1,4-NQ, sites other than the active site were very low populated and exhibit a less favorable energy of interaction (−2.73 kcal/mol).

The characterization of the energy of interaction between the enzyme and the inhibitors allows us to provide additional information about the most probable configuration for the complex, but in certain cases it cannot provide reliable data about the inhibitor selectivity or kinetic parameters. Free energies of binding and K_i values of human MAO-B docked with several inhibitors have been previously reported.[32] In this study, although the inhibitors are successfully docked onto the active site of MAO-B some discrepancies can be noted between the calculated and experimental K_i values. In our experiments, although the K_i for menadione and MAO-B was 60-fold lower than the K_i for menadione and MAO-A, the energies of interaction are quite similar for these isoforms. For competitive inhibition, the substrate and its energy of interaction with the active site of the enzyme will interfere with the affinity between the enzyme and inhibitor and will in turn affect K_i value. This type of competitive environment is not predicted in docking studies. Additionally, K_i values estimated from docking programs do not consider explicit water molecules during docking, and then solvation and entropic effects were not taken into account. Nevertheless, our docking data are consistent with the mechanisms for inhibition proposed based on the kinetic experiments. In case of menadione or 1,4-NQ with MAO-B, a interaction between the inhibitors and the FAD cofactor of enzyme was also verified by fluorescence experiments, corroborating to the hypothesis of a competitive mechanism for the inhibition.

3.4. Docking of TMN and MAO

Epidemiological data have revealed a lower incidence of PD in tobacco smokers (30–40%) compared to non-smokers.[33,34] One hypothesis suggests that this protection is a result of the reduced MAO-B and MAO-A activity in the smoker's brain.[35] In fact, previous studies have shown that tobacco smoke exposure leads to a 20% reduction in MAO-B activity in the mouse brain.[35] On the other hand, low levels of platelet MAO-B has been associated with personality traits linked to substance abuse vulnerability. Therefore, it remains unclear whether people are predisposed to become smokers as a result of low MAO-B activity or if the reduction in MAO-B activity is a result of exposure to tobacco substances. Although potential health hazards associated with tobacco products preclude any therapeutic approach linked to smoking, several investigations have attempted to isolate MAO inhibitors from tobacco. One of these inhibitors is TMN. We examined the structural features of MAO inhibition by TMN by using molecular docking. The energy of interaction of TMN with MAO-A and MAO-B in the lowest energy docked conformation was −6.27 and −6.39 kcal/mol, respectively, and occurs in the catalytic site of the enzymes (Fig. 5A and B, respectively). TMN interacts with the flavin moiety by a HB and by close contacts with the residues Tyr60, Leu171, Tyr326, Phe343, Tyr398 and Tyr435 in MAO-B active site. The enzyme residues involved in the interaction between MAO-A and TMN are quite similar to those involved in the 1,4-NQ interaction, with the exception of an additional interaction with Met350.

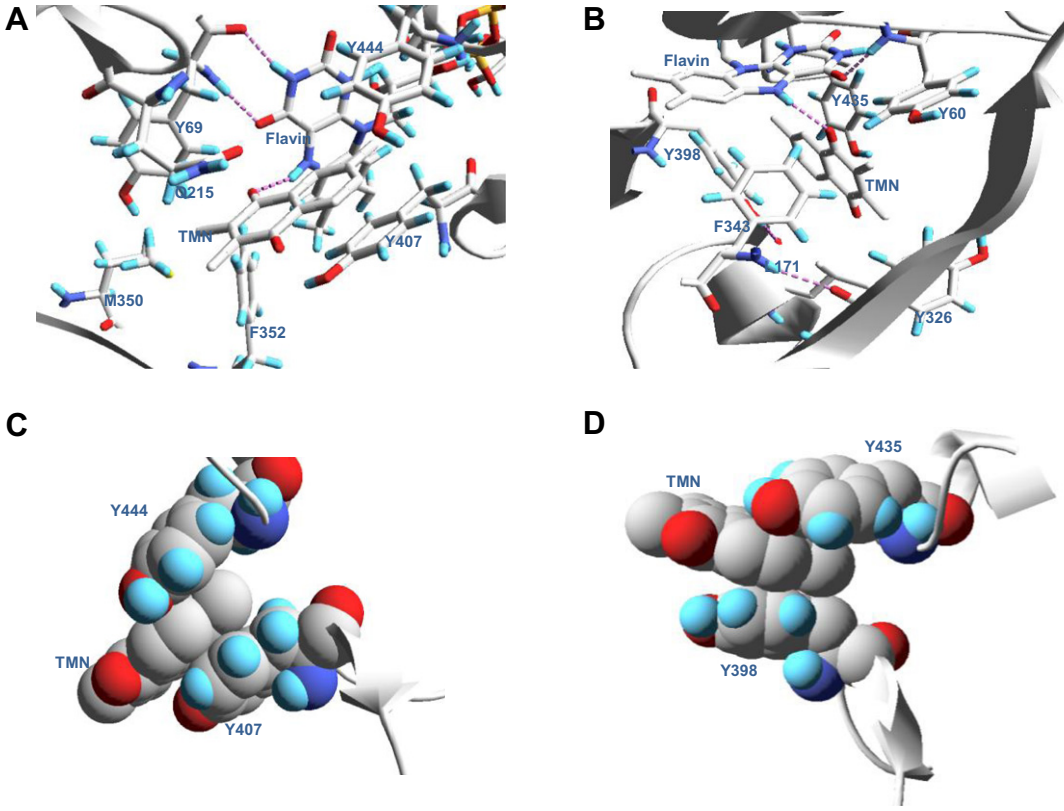

Figure 5. Interaction of TMN with MAO in the lowest energy docking conformation. The MAO-A residues that interact with TMN are quite similar to those that interact with 1,4-NQ, with exception of a additional interaction with Met350 (A). TMN interacts with the flavin moiety through a HB and close contact with Tyr60, Leu171, Tyr326, Phe343, Tyr398 and Tyr435 in the MAO-B active site (panel B). Dispersion forces with the phenyl side groups of Tyr407 and Tyr444 for MAO-A (C) or Tyr398 and Tyr435 for MAO-B (D) are suggest being responsible for a more favorable energy of interaction inhibitor-enzyme.

The analysis of the interactions in the lowest energy cluster configurations suggests that the phenyl side groups of Tyr407 and Tyr444 for MAO-A (Fig. 5C) or Tyr398 and Tyr435 for MAO-B (Fig. 5D) play an important role in the interaction with 1,4-NQ scaffold of TMN through forces of dispersion. Similar results were observed for 1,4-NQ and menadione. In addition, these residues are conserved in both MAO-A and MAO-B from different species.[36] In this conformation, the ligand is located between two tyrosine residues, perpendicularly to the *re* face of flavin moiety, which allows the phenolic side chains to form an 'aromatic sandwich' structure. Crystallographic data suggests that both inhibitors and substrates must pass between these two tyrosines to interact with the flavin group, making this 'aromatic sandwich' an important feature for enzyme functionality.[37] For rasagiline, an irreversible inhibitor of MAO-B, the aromatic moiety of the inhibitor interacts with the side chains of the residues of Tyr398 and Tyr435 in MAO-B structure while the residues Tyr60 and Phe343 are involved in the stabilization of the complex, similarly to observed with TMN and MAO-B.[32]

3.5. Reversibility and selectivity of MAO inhibitors in the therapy for neurological disorders

MAO inhibitors display a range of activities that may be a result of several factors beyond the increase of particular neurotransmitter levels. These factors include inhibition of the conversion of MPTP-like neurotoxins to their toxic metabolites (MAO-B converts MPTP to its neurotoxic form MPP^+), a reduction of reactive oxygen species generated from hydrogen peroxide (a product of MAO action) and anti-apoptotic activity.[37,38] In symptomatic therapy for PD, MAO inhibitors are used to increase neuronal dopamine (DA) levels. DA is metabolized by intraneuronal MAO-A and by MAO-A/MAO-B in glial and astrocyte cells.[38] Therefore, the selective inhibition of MAO-A or MAO-B does not change the steady state striatal DA levels. For instance, studies in rat brains show that the administration of selegiline or clorgiline does not produce a DA increase that is as significant as the increase observed for phenylethylamine, noradrenalin or serotonin.[39] The enhancement of DA release observed when a selective MAO inhibitor is administrated is likely associated with an increase in endogenous brain amines or the modulation of dopamine receptors.[8] In contrast, the administration of nonselective inhibitors of MAO-A/B, e.g. ladostigik, produces a very significant increase of DA levels.[40] Furthermore, nonselective inhibitors can increase levels of both DA and serotonin, which may be important in PD therapy as many patients also present symptoms of depression.[8] Our results suggest that 1,4-NQ may represent an important scaffold for design nonselective or weakly selective inhibitors acting on both isoforms of MAO. Menadione exhibited a clear preference for MAO-B with K_i value being significantly lower for MAO-B than MAO-A, resulting in a 60-fold selectivity for MAO-B as determined by the ratio $K_i^{MAO\text{-}A}/K_i^{MAO\text{-}B}$. The selectivity of menadione for human MAO-B is in the same range of rasagiline, an irreversible inhibitor of MAO-B (50-fold and 93-fold selectivity for human and rat MAO-B, respectively) but greatly lower than for selegiline (250-fold selectivity for human or rat MAO-B), a potent and irreversible MAO-B used in the clinic.[41]

The irreversible inhibition of MAO-A is associated with the potentialization of sympathetic cardiovascular activity through the release of noradrenaline.[42] This side effect occurs when tyramine, which is effectively metabolized by intestinal MAO-A, enter to circulation, resulting in noradrenaline release from sympathetic nerve endings and adrenaline from the adrenal gland. This side effect is known as the cheese-reaction because tyramine and other sympathomimetic amines are found in fermented foods and drinks, for example, cheese and beer. Therefore, hypertensive crises may be avoided by the use of reversible rather than irreversible MAO-A inhibitors. MAO-B inhibitors, especially those that are selective and irreversible, do not promote the cheese-reaction (unless administrated at doses high enough to inhibit MAO-A) because the intestine contains little MAO-B. Conversely, side effects associated with intestinal MAO-A inhibition might be avoided by using tissue-specific inhibitors such as the brain-selective ladostigil, even though the molecular basis of this selectivity remains unclear. Therefore, the reversibility exhibited by 1,4-naphthoquinones in MAO inhibition may be an attractive characteristic of these molecules in comparison to irreversible inhibitors by avoiding side effects associated with the cheese-reaction.

4. Conclusions

Our findings suggest that 1,4-NQ might represent an important scaffold for the development of MAO inhibitors. Computational and spectroscopy data suggest that 1,4-NQ as well as menadione or TMN interact with flavin ring in the catalytic site of MAO-B. Besides the catalytic site, another site of interaction, inside the enzyme, can be observed for MAO-A and 1,4-NQ, which is corroborated by the kinetic experiments that suggest a noncompetitive mechanism for 1,4-NQ and MAO-A. Menadione displays a 60-fold selectivity for MAO-B, similarly to rasagiline but significantly lower than selegiline or clorgyline, potent selective MAO inhibitors. Similar to certain MAO inhibitors, our data suggest that these 1,4-NQS are located between two tyrosine residues in the enzyme, perpendicularly to the *re* face of flavin moiety in a type of 'aromatic sandwich' structure. Taken together, our studies revealed that 1,4-NQs might behave as both reversible and nonselective inhibitors, even though the selectivity may be altered by changes in the substituents on the naphthoquinone ring.

Acknowledgements

This work was supported by Souza Cruz Co. and by *Fundação de Amparo à Pesquisa do Estado do Rio de Janeiro* (FAPERJ).

References and notes

1. Youdim, M. B.; Riederer, P. F. *Neurology* **2004**, *63*, 32.
2. Edmondson, D. E.; Binda, C.; Wang, J.; Upadhyay, A. K.; Mattevi, A. *Biochemistry* **2009**, *48*, 4220.
3. Javitch, J. A.; D'Amato, R. J.; Strittmatter, S. M.; Snyder, S. H. *Proc. Natl. Acad. Sci. U.S.A.* **1985**, *82*, 2173.
4. Bach, A. W.; Lan, N. C.; Johnson, D. L.; Abell, C. W.; Bembenek, M. E.; Kwan, S. W.; Seeburg, P. H.; Shih, J. C. *Proc. Natl. Acad. Sci. U.S.A.* **1988**, *85*, 4934.
5. Jenner, P. *Neurology* **2004**, *63*, 13.
6. Weinreb, O.; Mandel, S.; Bar-Am, O.; Yogev-Falach, M.; Avramovich-Tirosh, Y.; Amit, T.; Youdim, M. B. *Neurotheraphy* **2009**, *6*, 163.
7. Krishnan, K. R. *J. Clin. Psych.* **2007**, *68*, 35.
8. Youdim, M. B.; Bakhle, Y. S. *Br. J. Pharmacol.* **2006**, *147*, 287.
9. Maurel, A.; Hernandez, C.; Kunduzova, O.; Bompart, G.; Cambon, C.; Parini, A.; Francés, B. *Am. J. Physiol. Heart Circ. Physiol.* **2003**, *284*, 1460.
10. Fowler, J. S.; Logan, J.; Volkow, N. D.; Wang, G. J.; MacGregor, R. R.; Ding, Y. S. *Methods* **2002**, *27*, 263.
11. Lippman, S. B.; Nash, K. *Drug Saf.* **1990**, *5*, 195.
12. Khalil, A. A.; Steyn, S.; Castagnoli, N. *Chem. Res. Toxicol.* **2000**, *13*, 31.
13. Castagnoli, K. P.; Steyn, S. J.; Petzer, J. P.; Van der Schyf, C. J.; Castagnoli, N. J. *Chem. Res. Toxicol.* **2001**, *14*, 523.
14. Langston, J. W.; Langston, E. B.; Irwin, I. *Acta Neurol. Scand. Suppl.* **1984**, *100*, 49.
15. Thomson, R. H. *Naturally Occurring Quinones*; Springer: London, 1996.
16. Guang, H.; Du, G. *Acta Pharmacol. Sinica* **2006**, *27*, 760.
17. Dixon, M. *Biochem. J.* **1953**, *55*, 170.
18. Woo, J. C.; Silverman, R. B. *Biochem. Biophys. Res. Commun.* **1994**, *202*, 1574.
19. Dennington II, R.; Keith, T.; Millam, J. GaussView, Version 4.1, Semichem Inc., Shawnee Mission, 2007.
20. Frisch, M. J.; Trucks, G. W.; Schlegel, H. B.; Scuseria, G. E.; Robb, M. A.; Cheeseman, J. R.; Zakrzewski, V. G.; Montgomery Jr, J. A.; Stratmann, R. E.; Burant, J. C.; Dapprich, S.; Millam, J. M.; Daniels, A. D.; Kudin, K. N.; Strain, M. C.; Farkas, O.; Tomasi, J.; Barone, V.; Cossi, M.; Cammi, R.; Mennucci, B.; Pomelli, C.; Adamo, C.; Clifford, S.; Ochterski, J.; Petersson, G. A.; Ayala, P. Y.; Cui, Q.; Morokuma, K.; Salvador, P.; Dannenberg, J. J.; Malick, D. K.; Rabuck, A. D.; Raghavachari, K.; Foresman, J. B.; Cioslowski, J.; Ortiz, J. V.; Baboul, A. G.; Stefanov, B. B.; Liu, G.; Liashenko, A.; Piskorz, P.; Komaromi, I.; Gomperts, R.;

Martin, R. L.; Fox, D. J.; Keith, T.; Al-Laham, M. A.; Peng, C. Y.; Nanayakkara, A.; Challacombe, M.; Gill, P. M. W.; Johnson, B.; Chen, W.; Wong, M. W.; Andres, J. L.; Gonzalez, C.; Head-Gordon, M.; Replogle, E. S.; Pople, J. A. Gaussian 98 (Revision A.1x), Gaussian Inc., Pittsburgh, 2001.
21. Gasteiger, J.; Marsili, M. *Tetrahedron* **1980**, *36*, 3219.
22. Sanner, M. F. *J. Mol. Graph. Model* **1999**, *17*, 57.
23. Binda, C.; Wang, J.; Li, M.; Hubalek, F.; Mattevi, A.; Edmondson, D. E. *Biochemistry* **2008**, *47*, 5616.
24. Son, S. Y.; Ma, J.; Kondou, Y.; Yoshimura, M.; Yamashita, E.; Tsukihara, T. *Proc. Natl. Acad. Sci. U.S.A.* **2008**, *105*, 5739.
25. Morris, G. M.; Goodsell, D. S.; Halliday, R. S.; Huey, R.; Hart, W. E.; Belew, R. K.; Olson, A. J. *J. Comput. Chem.* **1998**, *19*, 1639.
26. Huey, R.; Morris, G. M.; Olson, A. J.; Goodsell, D. S. *J. Comput. Chem.* **2007**, *28*, 1145.
27. Binda, C.; Wang, J.; Pisani, L.; Caccia, C.; Carotti, A.; Salvati, P.; Edmondson, D. E.; Mattevi, A. *J. Med. Chem.* **2007**, *50*, 5848.
28. Herraiz, T.; Chaparro, C. *Biochem. Biophys. Res. Commun.* **2005**, *326*, 378.
29. Frei, B.; Winterhalter, K. H.; Richter, C. *Biochemistry* **1986**, *25*, 4438.
30. De Marchi, U.; Pietrangeli, P.; Marcocci, L.; Mondovì, B.; Toninello, A. *Biochem. Pharmacol.* **2003**, *66*, 1749.
31. Castillo, J.; Hung, J.; Rodriguez, M.; Bastidas, E.; Laboren, I.; Jaimes, A. *Anal. Biochem.* **2005**, *343*, 293.
32. Toprakçí, M.; Yelekçi, K. *Bioorg. Med. Chem. Lett.* **2005**, *15*, 4438.
33. Scott, W. K.; Zhang, F.; Stajich, J. M.; Scott, B. L.; Stacy, M. A.; Vance, J. M. *Neurology* **2005**, *64*, 442.
34. Gorell, J. M.; Rybicki, B. A.; Johnson, C. C.; Peterson, E. L. *Neurology* **1999**, *52*, 115.
35. Castagnoli, K.; Murugesan, T. *Neurotoxicology* **2004**, *25*, 279.
36. Nandigama, R. K.; Miller, J. R.; Edmondson, D. E. *Biochemistry* **2001**, *40*, 14839.
37. Nagatsu, T.; Sawada, M. *J. Neural. Transm. Suppl.* **2006**, *71*, 53.
38. Youdim, M. B.; Edmondson, D.; Tipton, K. F. *Nat. Rev. Neurosci.* **2006**, *7*, 295.
39. Riederer, P.; Youdim, M. B. *J. Neurochem.* **1986**, *46*, 1359.
40. Sagi, Y.; Driguès, N.; Youdim, M. B. *Br. J. Pharmacol.* **2005**, *146*, 553.
41. Youdim, M. B. H.; Gross, A.; Finberg, J. P. M. *Br. J. Pharmacol.* **2001**, *132*, 500.
42. Da Prada, M.; Zürcher, G.; Wüthrich, I.; Haefely, W. E. *J. Neural. Transm. Suppl.* **1988**, *26*, 31.